

AoCStream: All-on-Chip CNN Accelerator With Stream-Based Line-Buffer Architecture

Hyeong-Ju Kang

Korea University of Technology and Education
Cheonan, Chungcheongname-do, Republic of Korea
hjkang@koreatech.ac.kr

ABSTRACT

Convolutional neural network (CNN) accelerators are being widely used for their efficiency, but they require a large amount of memory, leading to the use of a slow and power consuming external memory. This paper exploits two schemes to reduce the required memory amount and ultimately to implement a CNN of reasonable performance only with on-chip memory of a practical device like a low-end FPGA. To reduce the memory amount of the intermediate data, a stream-based line-buffer architecture and a dataflow for the architecture are proposed instead of the conventional frame-based architecture, where the amount of the intermediate data memory is proportional to the square of the input image size. The architecture consists of layer-dedicated blocks operating in a pipelined way with the input and output streams. Each convolutional layer block has a line buffer storing just a few rows of input data. The sizes of the line buffers are proportional to the width of the input image, so the architecture requires less intermediate data storage than the conventional frame-based architecture, especially in the trend of getting larger input size in modern object detection CNNs. In addition to the reduced intermediate data storage, the weight memory is reduced by the accelerator-aware pruning. The experimental results show that a whole object detection CNN can be implemented even on a low-end FPGA without an external memory. Compared to previous accelerators with similar object detection accuracy, the proposed accelerator reaches much higher throughput even with less FPGA resources of LUTs, registers, and DSPs, showing much higher efficiency. The trained models and implemented bit files are available at <https://github.com/HyeongjuKang/accelerator-aware-pruning> and <https://github.com/HyeongjuKang/aocstream>.

CCS CONCEPTS

• **Hardware** → **Hardware accelerators**; Arithmetic and datapath circuits; *Application specific integrated circuits*.

KEYWORDS

CNN accelerator, object detection, on-chip memory, FPGA

1 INTRODUCTION

Recently, convolutional neural networks (CNNs) are showing great performances in computer vision tasks, including image recognition [10, 11, 27, 29], object detection [17, 18, 26, 28], and image segmentation [19]. However, CNNs usually require an enormous amount of memory and computation, so special hardware is usually adopted to implement them. Many kinds of CNN hardwares have been used, and a CNN accelerator in ASIC or FPGA shows high efficiency.

There have been many CNN accelerators [4, 13, 22, 30, 34], some of which focused on object detection [3, 7, 20, 23, 25, 31]. One of the main concerns in designing a CNN accelerator is how to reduce the number of external memory accesses. The processing of a CNN requires a large amount of memory, so the data are usually stored in an external memory like DRAM. Accessing an external DRAM consumes much power [9] and occupies long latency. Many previous CNN accelerators have proposed various data flows to reduce the number of external memory accesses.

To solve this problem and ultimately to implement a whole CNN model only with on-chip memory, there are two trivial solutions, embedding a large amount of on-chip memory [12, 21, 33] or using a very simplified CNN model [21]. However, these solutions are not so practical because of cost and degraded performance. It is still a challenging problem to reduce the required memory amount so that a CNN model of reasonable performance frequently used for embedded implementation [8, 32] can fit in the on-chip memory of a practical environment like a low-end or mid-range FPGA device.

In this paper, we reached this goal by adopting two approaches. The CNN processing stores two kinds of data in memory, the weights and the intermediate activation data. To reduce the amount of weight memory, we exploit the pruning scheme [6, 9, 16, 24], especially accelerator-aware pruning [14]. Pruning schemes can reduce the weight amount, but the irregularity leads to an inefficient implementation. The accelerator-aware pruning prunes weights considering the base accelerator, so it does not harm the accelerator performance.

To reduce the amount of the intermediate data memory, this paper proposes a stream-based line-buffer architecture. The main component of a CNN is a convolutional layer. The proposed architecture is specialized to process a convolutional layer, storing only a few rows of the intermediate data for each layer. A convolution is a local operation, so the calculation of an output activation requires only a few neighboring input data. If the input data are streamed into the processing block, only a few rows are required to be stored. To take full advantage of the line-buffer structure, a proper dataflow will be proposed, too. With the two schemes reducing the weight and the intermediate data memory, an object detection CNN can be implemented in a low-end FPGA without an external memory.

This paper is organized as follows. Section II introduces the basics of CNN computations, and Section III analyzes the memory sizes of CNN accelerators. The proposed architecture is described in Section IV, and the experimental results are shown in Section V. Section VI makes the concluding remarks.

2 CONVOLUTIONAL NEURAL NETWORKS

A CNN consists of many layers, which are stacked input-to-output. The data usually flow from input to output. The main layer in a CNN is a convolutional layer. A convolutional layer assumes N input feature maps whose height and width are H and W . A convolutional layer performs a convolution operation on the input feature maps as described in the following equation and produces M output feature maps, as follows.

$$fo(m, y, x) = \sum_{n=0}^{N-1} \sum_{i=0}^{K-1} \sum_{j=0}^{K-1} w(m, n, i, j) \times fi(n, S \times y + i, S \times x + j) + bias(m), \quad (1)$$

where $fi()$ and $fo()$ are a piece of the input and output feature map data, an input and output activation, respectively, and $w()$ is the weights.

To reduce the amount of weight and computation, a convolution layer can be divided into a depth-wise convolution and a point-wise convolution [11], where a point-wise convolution is a normal 1×1 convolution. In the depth-wise convolution, the number of the input feature maps, N , is equal to that of the output feature maps, M , and an output feature map is calculated from the corresponding input feature map.

$$fo(n, y, x) = \sum_{i=0}^{K-1} \sum_{j=0}^{K-1} w(n, i, j) \times fi(n, S \times y + i, S \times x + j) + bias(n) \quad (2)$$

CNNs are usually used for computer vision tasks including object detection. One of the most popular CNN types for object detection is the single-shot multi-box detector (SSD) [18]. The SSD exploits an image classification CNN like VGG, ResNet, and MobileNet as a base CNN. The feature maps shrink more with auxiliary layers, and the detection box information is generated through a few more layers. There are some SSD variants, and SSDLite [27] uses depth-wise convolutional layers instead of normal convolutional layers in the auxiliary part.

3 MEMORY SIZE OF CNN ACCELERATORS

One of the most important factors in designing CNN accelerators is the amount of required memories. Processing a neural network usually requires a huge amount of memories, usually larger than the amount that can be embedded on a low-end or mid-range FPGA. A CNN accelerator, therefore, usually uses external memories like DRAMs.

A CNN accelerator stores two types of data in memories, weights and intermediate activations. The amount of the weight memory is determined at the algorithm level by the CNN structure. The amount of the activation memory is also determined at the algorithm level, but it can be determined at the architecture level, too.

Traditionally, the memory amount for weights is believed to be much larger than that for the activations. In the traditional CNNs, however, most of the weights belong to the fully-connected layers [9]. The recent CNNs use only one or none fully-connected layers [10, 27], and the object detection CNNs do not use fully-connected layers at all [17, 18, 26]. In convolutional layers, the

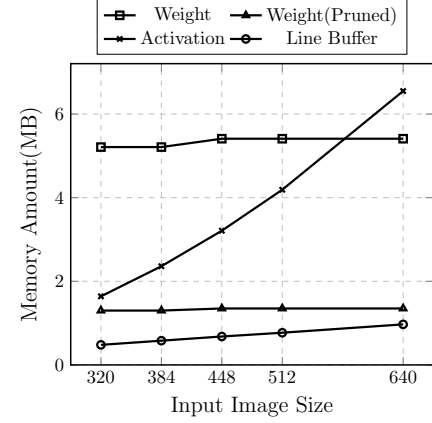


Figure 1: Memory amount for MobileNetV1 and SSDLiteX

memory requirement for weights is not much larger than that for activations, compared to those in fully-connected layers.

Furthermore, the activation amount is proportional to the square of the input image size. If the height and width of the input image are doubled, so are those of feature maps, and the activation amount increases by four-times. This is not a big problem when the target is the image classification because the input image size is usually very small, around 224. However, the modern object detection CNNs use large input images varying from 300 [18] to 1280 [28]. Considering the current trend of processing larger input images, the activation memory will become larger in the future.

The amount of the activation memory also depends on the accelerator architecture. In the conventional CNN accelerators, a neural network is processed layer by layer. A whole input feature map is stored in a memory, and a CNN accelerator reads activations from the memory, processes them, and stores the output activations. After generating the whole output feature maps, the CNN accelerator starts to process the next layer. Therefore, the CNN accelerator requires a memory for the whole input or output feature maps, and the amount is sometimes doubled for the double buffering. Some structures process a few layers at the same time [2, 4], but they store the intermediate data between the layer blocks, too.

To analyze the memory size, a few object detection CNNs were designed. The CNNs consist of MobileNetV1 [11] and SSDLiteX, a variant of SSDLite [27]. The CNNs are built for the images with various sizes from 320 to 640. The number of auxiliary layer stages changes with the input sizes. The input size 320 and 384 uses 4 stages, 448 and 512 uses 5 stages, and 640 uses 6 stages. The detailed CNN structure is provided in [15]. Figure 1 compares the memory amounts for each type of data with 8-bit quantization. For small input images, the memory amount for the activations (Activation in Figure 1) is around one-fourth of that for the weights (Weight in Figure 1). With large input images, the activations occupy almost the same memory as the weights do. If the double buffering scheme is applied, the intermediate activations require twice as large memories as that in the figure.

As another example of the state-of-the-art object detection CNNs, Figure 2 shows the memory requirement of EfficientDet [28], where the number of channels increases according to the input size. The

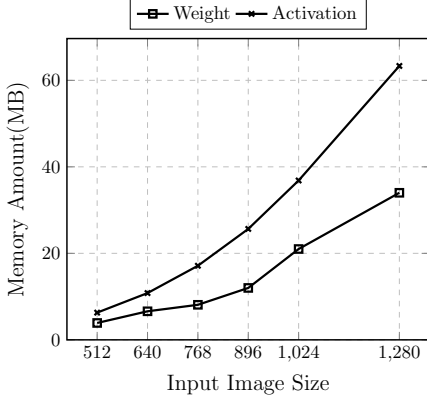


Figure 2: Memory amount for EfficientDet

amount of weights increases as input size is scaling up, but the amount of the activation memory is larger than that of the weight memory.

Furthermore, the weight amount can be reduced by pruning [6, 9, 14, 16, 24]. Recent research on pruning shows the amount of weight can be reduced by three fourths in convolutional layers [9, 14]. If the pruning is applied, the memory amount for weights is smaller than that for activations even with small input images, as shown in Figure 1. The pruning can reduce the weight amount, but there is no method to reduce the activation amount. The only way is using a smaller input image despite of the performance degradation or using another architecture.

4 STREAM-BASED LINE-BUFFER ARCHITECTURE

This paper follows the accelerator-aware pruning and the corresponding PE structure in [14] to reduce the weight amount, so the remaining part will focus on the reduction of the activation memory in the architecture and dataflow level, proposing a stream-based line-buffer accelerator architecture for CNNs.

4.1 Top architecture

The proposed accelerator processes a CNN in a layer-level pipelined way. Each layer has a corresponding processing block as shown in Figure 3. When a group of data is input to a block, the block processes the input data and generates a group of output data if possible. The generated group of data streams into the next block. Since each block does not wait for the previous block to complete the corresponding layer operation, all of the blocks can operate in parallel. The structure of a layer block is determined by the corresponding layer type.

4.2 Convolutional layer block

The base operation of a convolutional layer is the two-dimensional convolution. In the conventional image processing circuits, the two-dimensional convolution is usually processed by a stream-based structure with a line buffer of size $K-1$ lines. In the structure, the input data is assumed not to reside in a memory, but to stream in

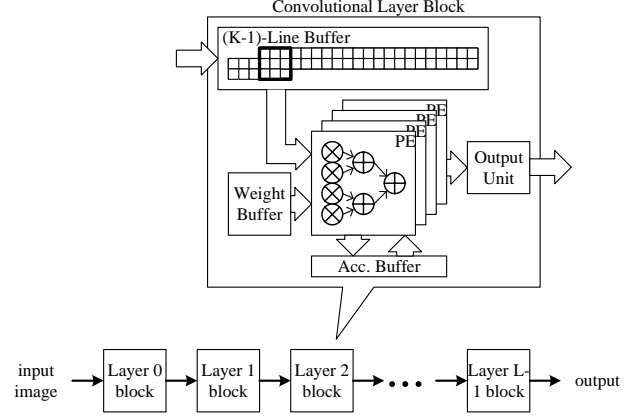


Figure 3: Stream-based line-buffer architecture

one by one. When one piece of input data streams in, the circuit processes the possible convolution operation.

The stream-based structure can be applied to the convolutional layer operation, but a proper dataflow is required to maintain the $K-1$ line-buffer size. As in the typical image processing circuits, it is assumed that the input data are streamed in the row-major order. For each spatial location, N channel data are divided into G_i groups, and a group of $N/G_i = N_i$ data is streamed-in together at the interval of I_i cycles as shown in Figure 4. With the N_i data, the layer block performs all of the computations that can be done with the input data and the data stored in the buffer. When g th group data, $fi(gN_i, y, x) \sim fi((g+1)N_i - 1, y, x)$, are input, the layer block calculates the following partial sums for each output $fo(m, Y, X)$, where $0 \leq m < M$, $Y = y - K + 1$, and $X = x - K + 1$. For simplicity, the stride S is assumed to be 1, but the structure is not limited to that.

$$fo_g(m, Y, X) = \sum_{n=gN_i}^{(g+1)N_i-1} \sum_{i=0}^{K-1} \sum_{j=0}^{K-1} w(m, n, i, j) \times fi(n, Y + i, X + j), \quad (3)$$

The partial sum requires $K \times K \times N_i \times M \times (1-r)$ MAC operations, where r is the pruning ratio, and the operations should be done in I_i cycles. Therefore, the required number of MAC operators is $K \times K \times N_i \times M_i \times (1-r)$, where $M_i = M/I_i$. The layer block has M_i processing elements (PEs), and a PE calculates a partial sum of an output with $K \times K \times N_i \times (1-r)$ multipliers at each cycle.

When a partial sum is calculated, it is accumulated with an accumulation buffer of size M . When all the data of a spatial location, $fi(n, y, x)$ for $0 \leq n < N$, are input through G_i groups, the calculation of the output data, $fo(m, Y, X)$ for $0 \leq m < M$, is completed through the accumulation. The output data are collected at the output unit and streamed out in G_o groups of $M/G_o = M_o$ data at the interval of I_o cycles. If the spatial size of the input feature maps is equal to that of the output feature maps, the following relationship should be satisfied.

$$\frac{N}{N_i} \times I_i \geq \frac{M}{M_o} \times I_o \quad (4)$$

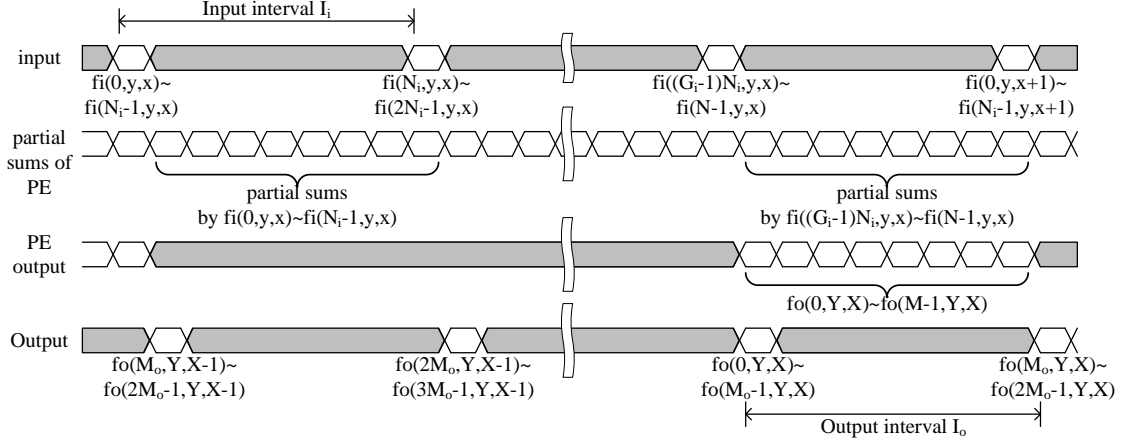


Figure 4: Convolutional layer processing

Some similar line-buffer structures were proposed for CNNs in [1, 3, 5, 21, 23, 35]. However, they did not employ a dataflow proper to the line-buffer structure. Their dataflow focuses on the weight data reuse, leading to the larger line-buffer of size K or $K+1$ lines. The large line-buffers make their accelerators use an external memory for the weights [23, 35] or require a very large FPGA device [3, 21].

On the contrary to the previous works, the proposed dataflow reuses the input feature map data as much as possible. After a $K \times K \times N_i$ input activation data block is gathered, the PEs perform all the computations related to the block. This dataflow property enables the line-buffer size of $K-1$ lines. However, this dataflow cannot reuse the weights, so it is proper to a structure with all of the weights in on-chip memory. With a weight memory reduction scheme, the proposed structure can exploit the dataflow to reduce the line-buffer size.

4.3 Depth-wise convolutional layer block

The depth-wise convolutional layer block also requires a line buffer of $(K-1)$ -line size as the convolutional layer block in the previous subsection. In the depth-wise convolution, the accumulation is not required between the input data groups. When $fi(gN_i, y, x) \sim fi((g+1)N_i-1, y, x)$ data are input, we can calculate $fo(gN_i, Y, X) \sim fo((g+1)N_i-1, Y, X)$. The required number of MAC operations is $K \times K \times N_i$. Each PE has one MAC unit and the number of PEs is determined as follows.

$$\text{Number of PEs} \geq \frac{K \times K \times N_i}{I_i} \quad (5)$$

4.4 Frame-buffer vs. line-buffer

When a CNN is processed layer-by-layer as in the conventional architecture, a frame buffer is required. For a layer l , a frame buffer of size $H_l \times W_l \times N_l$ is required for the input feature maps, and another of size $H_{l+1} \times W_{l+1} \times N_{l+1}$ is required for the output feature maps. Since a frame buffer can be reused between layers, the maximum size is required as follows.

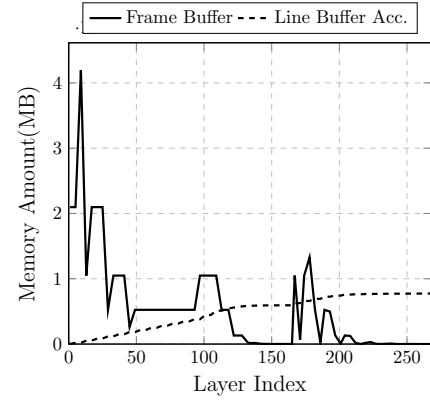


Figure 5: Frame-buffer vs. line-buffer

$$\text{Frame Buffer Size} = \max_l H_l \times W_l \times N_l \quad (6)$$

In the proposed architecture, a line buffer is used for each convolutional layer block, depth-wise convolutional layer block, and pooling layer block. Since the blocks operate in parallel, the line buffers cannot be shared. Therefore, the total size of the line buffers is as follows.

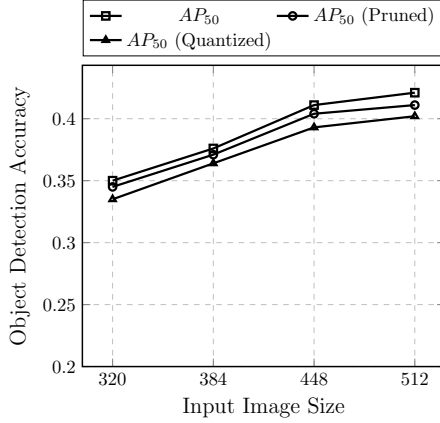
$$\text{Line Buffer Size} = \sum_l (K_l - 1) \times W_l \times N_l \quad (7)$$

When the input image size is scaled-up, the input image is enlarged vertically and horizontally. The frame buffer size in (6) is increased with the square of the scale. Contrary to that, the line buffer size in (7) has only the width term, W_l . The line buffer size is proportional to the scale linearly. In Figure 1, the frame buffer size is shown as *Activation*, which increases rapidly with the input image size. However, the line buffer size, denoted as *Line Buffer*, increases slowly with the input image size.

Figure 5 compares the frame buffer size and the accumulated line buffer in each layer of MobileNetV1 and SSDLiteX with 512×512

Table 1: FPGA Implementation Results

Architecture	[31]	[7]	[23]	AoCStream (Proposed)					
CNN	MNetV1+SSD	MNetV2+SSDLite	YOLOv3	MNetV1 + SSDLiteX					
Input Size	320	224	416	320	384	448	512	320	448
MS COCO AP	.193	.203	.310	.211	.231	.247	.253	.206	.247
FPGA	XCZU9EG	ZC706	XC7VX485T	XCKU5P				XC7K325T	XC7VX485T
LUT(K)	162	148	230	137	145	148	154	155	154
Reg(K)	301	192	223	218	219	233	232	195	237
BRAM	771	311	972.5	454	454	476	476	445	648
URAM	-	-	-	25	25	25	44	-	-
DSP	2070	728	2640	464	464	476	476	360	476
Clock(MHz)	333	100	200	428	349	400	375	186	223
Throughput(FPS)	124.3	15.4	11.66	260.9	147.7	124.5	89.3	100.9	69.5
DSP Efficiency 1(%)	22.3	8.3	-	80.2	80.2	78.3	78.3	76.1	78.3
DSP Efficiency 2(%)	-	-	72.4	289	289	282	282	332	282
Ext. Mem.	WA	WA	W	None	None	None	None	None	None

**Figure 6: Object detection accuracy for MS COCO dataset**

input image. The maximum size of the frame buffer is 4M at the output of the first point-wise convolution. The line buffer in each layer is very small, so it would not be clearly shown in the figure. Instead of the line buffer size in each layer, the figure illustrates the accumulated line buffer amount, which is less than one fourth of the frame buffer size.

4.5 All-on-chip accelerator

The weight pruning and the line buffer architecture reduces the storage of the weights and the intermediate data, respectively, so their combination can lead to all-on-chip implementation. The two schemes can reduce the memory size by around three-fourths. For example, the 512×512 input image case in Figure 1 requires the weight memory of around 5MB and the intermediate data memory of around 4MB. The total memory requirement of 9MB cannot be afforded by a low-end or mid-range FPGA device like Xilinx XCKU5P, whose on-chip memory size is 4MB. If the two schemes are applied, the total memory size becomes around 2.3MB, which is less than the on-chip memory size of XCKU5P.

The proposed scheme does not guarantee that any CNN can be implemented only with the on-chip memory of any device. There will be no such scheme. The proposed scheme, however, broadens the possibility of the all-on-chip implementation, higher performance CNNs on smaller devices.

5 EXPERIMENTAL RESULTS

Object detection CNNs based on MobileNetV1 and SSDLiteX with various input sizes are trained and implemented with the proposed architecture. The CNNs are trained with the MS COCO data set and pruned by the accelerator-aware pruning. The pruning ratio is 75%, which means 6 weights are pruned for every 8 weights along the channel axis. The pruned CNNs are quantized with 8–10 bits without fine-tuning. The object detection accuracy, AP_{50} , for the MS COCO dataset is provided after each step of training, pruning, and quantization in Figure 6. Pruning and quantization degrade AP_{50} by around 0.01–0.02, but the detection accuracy is still high for such compact CNNs. If retraining is applied with quantization, better detection accuracy could be obtained. The final AP values are shown at the fourth row of Table 1.

The proposed accelerator is designed in the register-transfer level (RTL) for the quantized CNNs and implemented for a low-end Xilinx FPGA, XCKU5P, which is the second smallest device in the UltraScale+ Kintex series. The implementation results are shown on the right side of Table 1. The table shows the occupancy of FPGA resources including look-up tables (LUT), registers, block memories (BRAM), ultra memories (URAM), and DSP units. The last two columns are the implementation results for older FPGAs, Kintex-7 series and Virtex-7 series, for comparison with previous works. Because of the resource limitation, some layers are pruned to 87.5% for XC7K325T.

The last four rows of the table show the operating clock frequency, the throughput in frames per second, the DSP efficiency, and the external memory use. The DSP efficiency is calculated as

follows.

$$\text{DSP Efficiency } 1 = \frac{(\text{Operations/Frame}) \times (\text{Frames/second})}{2 \times (\text{Num. of DSPs}) \times (\text{Clock Freq.})} \quad (8)$$

, where the $2\times$ in the denominator reflects that a DSP can process two operations, a multiplication and an addition, simultaneously. The second DSP efficiency is the effective efficiency, which includes the zero-skipped operations in a sparsity architecture, so the effective efficiency can be higher than 100% if pruning is applied. At the last *Ext. Mem.* row, W and A means the weights and the activations are stored in external memories, respectively. As the table shows, the proposed architecture can store the whole intermediate data and weights on the on-chip BRAM and URAM even for the input image size 512×512 . The all-on-chip implementation leads to high throughput and efficiency. The architecture can process images in 90 to 250 fps, which is much faster than the real-time speed, 30fps.

The table also compares the proposed architecture with the previous ones. The architectures of the second and third columns use CNNs similar to the one used in this paper. The accelerator of [31] used the MobileNetV1 and SSD combination. Their architecture shows the highest throughput in the previous ones, but it is slower even with around five-times more DSPs than the proposed architecture of the same input size. The architecture of the third column used MobileNetV2 and SSDLite with a small input size [7]. Despite of such small input size and high DSP usage, the throughput is very low. The accelerators of [31] and [7] are based on the frame-based architecture, so their DSP efficiency is very low because of the DRAM accesses. At the fourth column, an accelerator using YOLOv3 is compared [23]. The accelerator exploits a line buffer architecture similar to the proposed one, but it uses a larger line buffer in each layer and still needs an external memory for weights. Because they used a different CNN, it is difficult to compare their accelerator with the proposed one, but the DSP efficiency is lower than AoCStream. Even though they adopted a sparsity architecture, the effective DSP efficiency is not higher than 100% probably because of DRAM accesses for weights. HPIPE proposed in [3] also used a line buffer architecture, but it is implemented on a different type of FPGA. Because of the different internal FPGA structure, it is not compared in the table. However, HPIPE uses much resource to implement a similar object detection CNN, 4,434 DSPs and 7,179 M20K BRAMs for MobileNet v1 and SSD, showing less-than-50% DSP efficiency.

6 CONCLUSION

In this paper, object detection CNNs with reasonable performance were implemented only with the on-chip memory of a practical device. The memory amount is reduced in the algorithm level, accelerator-aware pruning, and in the architecture level, a stream-based line buffer architecture. In the architecture, a dedicated block is assigned to each layer, and the layer blocks operate in a pipelined way. The intermediate data are streamed into and out of each block, so only a few rows are stored in each block thanks to the property of the convolution operation. The reduction of the intermediate data storage is combined with the reduction of the weight storage by pruning to remove the need of external memories. The all-on-chip implementation greatly enhances the performance of the CNN

accelerator. The architecture can be applied to various CNNs for other computer vision tasks.

REFERENCES

- [1] Thea Aarrestad et al. 2021. Fast convolutional neural networks on FPGAs with hls4ml. *Machine Learning: Science and Technology* 2, 4, Article 045015 (Jul 2021), 24 pages.
- [2] Manoj Alwani, Han Chen, Michael Ferdman, and Peter Milder. 2016. Fused-Layer CNN Accelerators. In *Proceedings of International Symposium on Micro-architecture*.
- [3] Anupreetham Anupreetham et al. 2021. End-to-End FPGA-based Object Detection Using Pipelined CNN and Non-Maximum Suppression. In *Proceedings of International Conference on Field Programmable Logic and Applications*. 76–82.
- [4] Lin Bai, Yiming Zhao, and Xinming Huang. 2018. A CNN accelerator on FPGA using depthwise separable convolution. *IEEE Transactions on Circuits and Systems-II: Express Briefs* 65, 10 (Oct. 2018), 1415–1419.
- [5] Michaela Blott et al. 2018. FINN-R: An End-to-End Deep-Learning Framework for Fast Exploration of Quantized Neural Networks. *ACM Trans. Reconfigurable Technol. Syst.* 11, 3, Article 16 (Dec 2018), 23 pages.
- [6] Yoonho Boo and Wonyong Sung. 2017. Structured sparse ternary weight coding of deep neural networks for efficient hardware implementations. In *Proceedings of IEEE Workshop on Signal Processing Systems Design and Implementation*.
- [7] Hongxiang Fan et al. 2018. A real-time object detection accelerator with compressed SSDLite on FPGA. In *Proceedings of International Conference on Field Programmable Technology*. 17–24.
- [8] Google Inc. 2022. *Coral Object Detection Models*. <https://coral.ai/models/object-detection>
- [9] S. Han, H. Mao, and W. J. Dally. 2016. Deep Compression: Compressing deep neural networks with pruning, trained quantization and Huffman coding. In *Proceedings of International Conference on Learning Representations*. <http://arxiv.org/abs/1510.00149>
- [10] K. He, X. Zhang, S. Ren, and J. Sun. 2016. Deep residual learning for image recognition. In *Proceedings of IEEE/CVF Conference on Computer Vision and Pattern Recognition*. 770–778. <http://arxiv.org/abs/1512.03385>
- [11] Andrew G. Howard et al. 2017. *MobileNets: Efficient Convolutional Neural Networks for Mobile Vision Applications*. <http://arxiv.org/abs/1704.04861>
- [12] Yang Jiao et al. 2020. A 12nm Programmable Convolution-Efficient Neural-Processing-Unit Chip Achieving 825TOPS. In *Proceedings of IEEE International Solid-State Circuits Conference*. 136–137.
- [13] Jihyuck Jo, Soyoung Cha, Dayoung Rho, and In-Cheol Park. 2018. DSIP: A scalable inference accelerator for convolutional neural networks. *IEEE Journal of Solid-State Circuits* 53, 2 (Feb. 2018), 605–618.
- [14] Hyeon-Ju Kang. 2020. Accelerator-Aware Pruning for Convolutional Neural Networks. *IEEE Transactions on Circuits and Systems for Video Technology* 30, 7 (July 2020), 2093–2103. <https://doi.org/10.1109/TCSVT.2019.2911674>
- [15] Hyeon-Ju Kang. 2022. *Accelerator-aware pruning*. <https://github.com/HyeonjuKang/accelerator-aware-pruning>
- [16] Jiajun Li and Ahmed Louri. 2022. AdaPrune: An accelerator-aware pruning technique for sustainable CNN accelerators. *IEEE Transactions on Sustainable Computing* 7, 1 (Jan 2022), 47–60.
- [17] Tsung-Yi Lin, Piotr Dollár, Ross Girshick, Kaiming He, Bharath Hariharan, and Serge Belongie. 2017. Feature pyramid networks for object detection. In *Proceedings of IEEE/CVF Conference on Computer Vision and Pattern Recognition*. 936–944.
- [18] Wei Liu, Dragomir Anguelov, Dumitru Erhan, Christian Szegedy, Scott Reed, Cheng-Yang Fu, and Alexander C. Berg. 2016. SSD: Single shot multibox detector. In *Proceedings of European Conference on Computer Vision*. <http://arxiv.org/abs/1512.02325>
- [19] Jonathan Long, Evan Shelhamer, and Trevor Darrell. 2015. Fully convolutional networks for semantic segmentation. In *Proceedings of IEEE/CVF Conference on Computer Vision and Pattern Recognition*. 3431–3440. <http://arxiv.org/abs/1411.4038>
- [20] Ying-Cheng Lu et al. 2021. An 176.3 GOPs object detection CNN accelerator emulated in a 28nm CMOS technology. In *Proceedings of IEEE International Conference on Artificial Intelligence Circuits and Systems*. 1–4.
- [21] Jian Meng et al. 2021. FixyFPGA: Efficient FPGA Accelerator for Deep Neural Networks with High Element-Wise Sparsity and without External Memory Access. In *Proceedings of International Conference on Field Programmable Logic and Applications*. 9–16.
- [22] Seungsik Moon, Hyunhoon Lee, Younghoon Byun, Jongmin Park, Junseo Joe, Seokha Hwang, Sunggu Lee, and Youngjoo Lee. 2019. FPGA-based sparsity-aware CNN accelerator for noise-resilient edge-level image recognition. In *Proceedings of IEEE International Solid-State Circuits Conference*. 205–208.
- [23] Dyu Thanh Nguyen, Hyun Kim, and Hyuk-Jae Lee. 2021. Layer-specific optimization for mixed data flow with mixed precision in FPGA design for CNN-based object detectors. *IEEE Transactions on Circuits and Systems for Video Technology*

- 31, 6 (June 2021), 2450–2464.
- [24] Wei Pang, Chenglu Wu, and Shengli Lu. 2020. An energy-efficient implementation of gorup pruned CNNs on FPGA. *IEEE Access* 8 (2020), 217033–217044.
- [25] Daniel Pestana et al. 2021. A full featured configurable accelerator for object detection with YOLO. *IEEE Access* 9 (2021), 75864–75877.
- [26] Joseph Redmon and Ali Farhadi. 2018. *YOLOv3: An incremental improvement*. <http://arxiv.org/abs/1804.02767>
- [27] Mark Sandler, Andrew Howard, Menglong Zhu, Andrey Zhmoginov, and Liang-Chieh Chen. 2018. MobileNetV2: Inverted residuals and linear bottlenecks. In *Proceedings of IEEE/CVF Conference on Computer Vision and Pattern Recognition*. 4510–4520. <http://arxiv.org/abs/1801.04381>
- [28] Mingxing Tan, Ruoming Pang, and Quoc V. Le. 2020. EfficientDet: Scalable and efficient object detection. In *Proceedings of IEEE/CVF Conference on Computer Vision and Pattern Recognition*. 10778–10787.
- [29] Mingxing Tan and Quoc V. Le. 2019. EfficientNet: Rethinking model scaling for convolutional neural networks. In *Proceedings of International Conference on Machine Learning*.
- [30] Jiayu Wen, Yufei Ma, and Zhongfeng Wang. 2020. An efficient FPGA accelerator optimized for high throughput sparse CNN inference. In *Proceedings of IEEE Asia Pacific Conference on Circuits and Systems*. 165–168.
- [31] Di Wu, Yu Zhang, Xijie Jia, Lu Tian, Tianping Li, Lingzhi Sui, Dongliang Xie, and Yi Shan. 2019. A High-Performance CNN Processor Based on FPGA for MobileNets. In *Proceedings of International Conference on Field Programmable Logic and Applications*. 136–143.
- [32] Xilinx Inc. 2022. *Xilinx AI Model Zoo*. https://github.com/Xilinx/Vitis-AI/tree/master/model_zoo
- [33] Tian Yuan, Weiqiang Liu, Jie Han, and Fabrizio Lombardi. 2021. High Performance CNN Accelerators Based on Hardware and Algorithm Co-Optimization. *IEEE Transactions on Circuits and Systems-I: Regular Papers* 68, 1 (Jan. 2021), 250–263.
- [34] Chen Zhang, Peng Li, Guangyu Sun, Yijin Guan, Bingjun Xiao, and Jason Cong. 2015. Optimizing FPGA-based accelerator design for deep convolutional neural networks. In *Proceedings of ACM/SIGDA International Symposium on Field Programmable Gate Arrays*. 161–170.
- [35] Xiaofan Zhang, Junsong Wang, Chao Zhu, Yonghua Lin, Jinjun Xiong, Wen-mei Hwu, and Deming Chen. 2018. DNNBuilder: An Automated Tool for Building High-Performance DNN Hardware Accelerators for FPGAs. In *Proceedings of International Conference on Computer Aided Design*. 1–8.